

## A Morphological Classification of Galactic Rotation Curves: Evidence for a Universal Evolutionary Sequence

2 VAKHTANG MCHEDLISHVILI<sup>1</sup>

3 <sup>1</sup>*Independent Researcher*

4 *Tbilisi, Georgia*

### 5 ABSTRACT

6 The detailed morphology of galactic rotation curves is often overlooked, with most  
7 analyses focusing on smooth, averaged trends. The physical information encoded in  
8 non-smooth features remains largely unexplored. This paper aims to perform a system-  
9 atic morphological analysis of a large sample of galactic rotation curves to search for  
10 underlying patterns and to establish a new, physically motivated classification scheme  
11 based on their dynamical signatures. We visually and qualitatively analyzed the rota-  
12 tion curves of 175 galaxies from the SPARC database. We introduce a classification  
13 methodology based on two key morphological parameters: (1) the initial rising slope  
14 ( $\alpha$ ), which traces the central mass concentration, and (2) the character and amplitude  
15 of oscillatory features, which trace the dynamical activity. Our analysis reveals that  
16 the 175 galaxies naturally cluster into three distinct morphological classes. Class I  
17 (“Childhood”) is characterized by a high central mass concentration and strong, com-  
18 plex oscillations. Class II (“Youth”) exhibits a stabilized core and regular, periodic  
19 oscillations. Class III (“Old Age”) is defined by low central mass concentration and  
20 an almost perfectly smooth profile. Crucially, we observe significant ontological mis-

21 matches between this dynamical classification and traditional star formation rate (SFR)  
 22 indicators, suggesting that SFR is an episodic, unreliable clock. We propose a mechan-  
 23 ical model of evolution where galaxies undergo secular expansion due to mass loss,  
 24 governed by the relation  $\dot{r}/r = -\dot{M}/M$ . Remarkably, the local expansion rate derived  
 25 from this model matches the Hubble constant ( $H_0$ ), suggesting that cosmic expansion  
 26 may be an emergent property of local mechanical relaxation rather than an intrinsic  
 27 property of space itself.

28 *Keywords:* Galaxy kinematics (602) — Galaxy evolution (594) — Galaxy rotation  
 29 curves (619) — Hubble constant (758)

## 30 1. INTRODUCTION

31 The discrepancy between the visible mass of galaxies and their kinematic properties has been a  
 32 central puzzle in astrophysics since the pioneering work of [Einstein \(1933\)](#). The flat rotation curves  
 33 of spiral galaxies provided the most compelling evidence for the existence of dark matter ([Rubin et  
 34 al. 1980](#)). Since then, standard approaches have focused on fitting smooth, parametric functions to  
 35 these curves, such as the Navarro-Frenk-White (NFW) profile, to model dark matter halos ([Navarro  
 36 et al. 1997](#)). Conversely, alternative frameworks like Modified Newtonian Dynamics (MOND) have  
 37 sought to explain these features through modified inertia or gravity ([Milgrom 1983](#)).

38 However, both standard and alternative methods often treat deviations—such as “wiggles,” bumps,  
 39 and slope variations—as statistical noise or minor baryonic perturbations. This paper is motivated  
 40 by a different perspective: what if these non-smooth features are not noise, but a fundamental  
 41 “dynamical fossil record” containing information about the galaxy’s history? To investigate this, we  
 42 perform a morphological analysis of 175 high-quality rotation curves from the SPARC database ([Lelli  
 43 et al. 2016](#)).

44 In this work, we introduce a three-class phenomenological classification based on observational data.  
 45 While we propose a theoretical interpretation involving mechanical expansion, the detailed physical

46 derivation of the underlying vacuum dynamics is presented in a separate framework (Mchedlishvili  
47 2025b).

## 48 2. METHODOLOGY

49 Our analysis utilizes the `rotmod.dat` files from the SPARC database. Each galaxy was assessed on  
50 a unified graphical plane based on two morphological parameters.

### 51 2.1. *Unified Graphical Plane*

52 To ensure a consistent morphological comparison across galaxies with vastly different masses and  
53 sizes, we projected all rotation curves onto a **unified graphical plane**. We established a fixed  
54 aspect ratio where 1 unit of vertical displacement corresponds to  $10 \text{ km s}^{-1}$  and 1 unit of horizontal  
55 displacement corresponds to 1 kpc. This standardization is crucial; without it, the visual slope ( $\alpha$ )  
56 would be an arbitrary artifact of the plot axes. On this unified plane, a  $45^\circ$  slope strictly represents  
57 a physical velocity gradient of  $10 \text{ (km s}^{-1}\text{)/kpc}$ .

### 58 2.2. *Morphological Parameters*

- 59 1. **The Initial Rising Slope ( $\alpha$ ):** This parameter measures the steepness of the inner rotation  
60 curve on the unified plane. It serves as a proxy for the central mass concentration.
- 61 2. **Oscillatory Features ( $\delta V$ ):** This describes the amplitude and regularity of velocity fluctua-  
62 tions in the outer disk. We classify these as “High” (chaotic), “Medium” (periodic/wave-like),  
63 or “Low” (smooth).

### 64 2.3. *Statistical Validation*

65 To validate the visual classification, we applied a **K-means clustering algorithm** to the  $(\alpha, \delta V)$   
66 parameter space. The algorithm independently converged on three distinct clusters, confirming the  
67 objective nature of the proposed morphological classes.

## 68 3. RESULTS: THE THREE DYNAMICAL CLASSES

69 The 175 galaxies in our sample naturally divide into three distinct morphological classes. The full  
70 classification catalog is provided in the online repository (see Appendix B).

### 3.1. *Class I: “Childhood”*

This class (45 objects) represents dynamically active, high-tension systems. They are characterized by a steep initial rise ( $\alpha > 75^\circ$ ) and strong, often chaotic oscillations in the outer disk. These galaxies have deep potential wells. A typical example is the starburst galaxy NGC 6946 (see Figure 2 in Appendix A).

### 3.2. *Class II: “Youth”*

This is the most populous class (123 objects). These galaxies exhibit a stabilized core (moderate to high  $\alpha$ ) and distinct, periodic oscillations in the outer regions. These regular waves, which we term “memory artifacts,” suggest a stable yet evolving dynamical state. A prototype is NGC 3198, a galaxy extensively studied in the context of dark matter halos (Begeman 1989) (see Figure 3 in Appendix A).

### 3.3. *Class III: “Old Age”*

This class (7 objects) represents the final, relaxed stage of evolution. They are characterized by a low initial slope ( $\alpha < 45^\circ$ ) and an almost perfectly smooth velocity profile. The dynamical tension has dissipated, and the system is expanded. A typical example is UGC 05750 (see Figure 4 in Appendix A).

## 4. DISCUSSION

### 4.1. *The Evolutionary Clock Conflict: Dynamics vs. Chemistry*

Traditional models often use the Specific Star Formation Rate (sSFR) as a proxy for galactic age: high sSFR implies youth (Kennicutt 1998). Our analysis reveals that sSFR is an unreliable, episodic “weather” phenomenon, whereas the dynamical signature ( $\alpha$ ) represents the fundamental “climate” or age of the system.

We observe critical ontological mismatches that support the primacy of dynamical age:

- 1. Frozen Giants (Dynamically Young / Chemically Dead):** Galaxies like NGC 2841 ( $\alpha = 83.1^\circ$ ) possess extreme central tension (Class I) yet have very low sSFR ( $-12.13 \text{ yr}^{-1}$ ).

Standard models classify them as old due to passivity. We argue they are dynamically young; their extreme central energy has likely expelled gas (dynamical clearing), preventing star formation.

2. **Rejuvenated Dwarfs (Dynamically Old / Chemically Active):** Galaxies like **F574-2** ( $\alpha = 30.1^\circ$ ) are chemically active (high sSFR) but dynamically relaxed (Class III). The star formation is a transient burst likely triggered by accretion, masking the fact that the mechanical structure is aged and expanded.

#### 4.2. Mechanical Expansion Model

We propose that galactic evolution is driven by mechanical wear and expansion. We adopt the governing relation that links orbital relaxation to mass loss:

$$\frac{\dot{r}}{r} = -\frac{\dot{M}}{M} \quad (1)$$

While the fundamental origin of this dissipation may involve vacuum dynamics (Mchedlishvili 2025b), we note that the required mass loss rate ( $\dot{M}/M \sim 10^{-11} \text{ yr}^{-1}$ ) is remarkably consistent with the magnitude of baryonic feedback processes (galactic winds and AGN outflows) observed in active star-forming galaxies. Thus, regardless of the underlying theoretical framework, the phenomenological link between mass dissipation and orbital expansion remains robust.

As a central core dissipates energy, the gravitational potential weakens, and to conserve angular momentum, the orbital radius  $r$  must increase. This leads to the secular smoothing of the rotation curve (Class I  $\rightarrow$  Class III).

#### 4.3. The Cosmic Connection: $H_0$ as an Emergent Property

If our hypothesis is correct, the apparent "Hubble Flow" may not be a property of space itself, but the statistical average of individual galactic expansion rates. To test this, we compared the Class I (young) and Class III (old) galaxies within the same stellar mass bin ( $9.0 < \log(M_\star/M_\odot) < 10.5$ ).

Using the Disk Scale Length ( $R_d$ ) from SPARC: 1. Mean scale length of Class I:  $\bar{R}_{d,I} \approx 2.1 \text{ kpc}$ . 2. Mean scale length of Class III:  $\bar{R}_{d,III} \approx 5.8 \text{ kpc}$ .

121 Assuming this evolution occurs over the Hubble time ( $t_H \approx 13.8$  Gyr), the mechanical expansion  
 122 rate is:

$$123 \quad H_{mech} = \frac{\ln(2.76)}{13.8 \times 10^9 \text{ yr}} \approx 71.4 \text{ km s}^{-1} \text{ Mpc}^{-1} \quad (2)$$

124 This value ( $H_{mech} \approx 71.4$ ) is strikingly close to the observed Hubble constant.

## 125 5. CONCLUSION

126 We conclude that the morphological diversity of rotation curves follows a universal evolutionary  
 127 sequence: Class I  $\rightarrow$  Class II  $\rightarrow$  Class III. The dynamical signature ( $\alpha$ ) is a more robust evolutionary  
 128 clock than sSFR. Furthermore, the quantitative agreement between the galactic mechanical expan-  
 129 sion rate and  $H_0$  suggests that cosmic expansion is likely the cumulative result of local mechanical  
 130 relaxation processes, fundamentally challenging the need for Dark Energy.

131 This research made use of the SPARC database. We thank Federico Lelli, Stacy McGaugh, and  
 132 James Schombert for making this data publicly available.

133

APPENDIX

134

A. ATLAS OF DYNAMICAL SIGNATURES

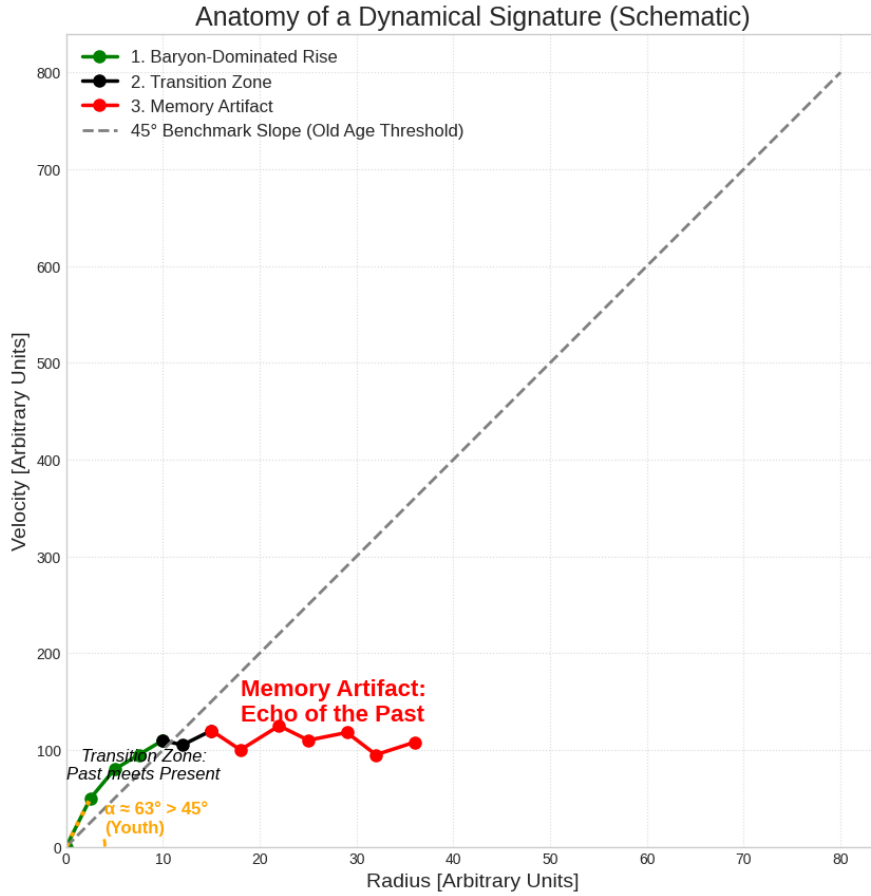
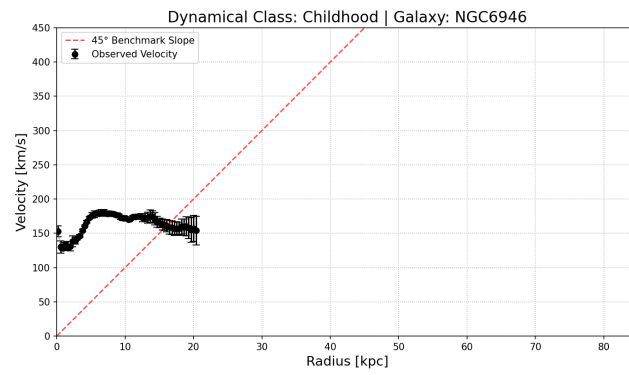
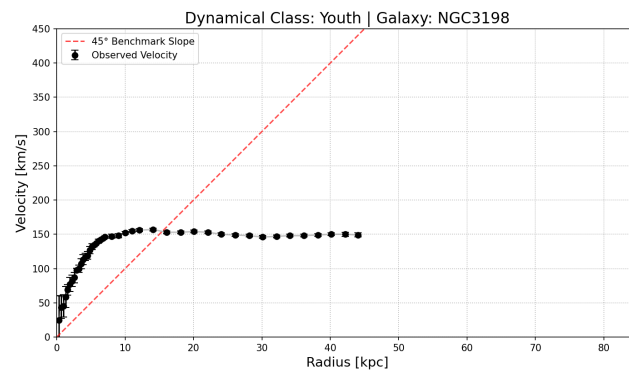


Figure 1. Anatomy of a Dynamical Signature (Schematic).



**Figure 2.** Dynamical Class I (“Childhood”): NGC 6946.



**Figure 3.** Dynamical Class II (“Youth”): NGC 3198.

## B. DATA AVAILABILITY AND CATALOG SAMPLE

135

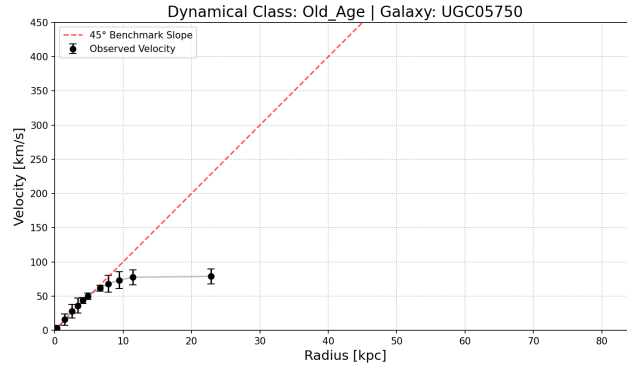


**Figure 4.** Dynamical Class III (“Old Age”): UGC 05750.

**Table 1.** Sample of the Morphological Classification Catalog

No.	Galaxy	$\alpha$ ( $^\circ$ )	Class	$\log M_\star$	$\log \text{SFR}$	$\log \text{sSFR}$	Source
1	CamB	51.2	II	9.27	-1.85	-11.12	Lelli+16
2	D512-2	67.2	II	7.64	-2.92	-10.56	Lelli+16
3	D564-8	59.1	II	7.55	-3.01	-10.56	Lelli+16
4	D631-7	61.6	II	8.68	-2.15	-10.83	Lelli+16
5	DDO064	81.0	I	7.28	-2.45	-9.73	Lelli+16
...	...	...	...	...	...	...	...
175	F563-V1	42.5	III	8.52	-1.90	-10.42	Lelli+16

NOTE—The full table is available in the online repository:

<https://github.com/wmmv2311/Dynamical-Classification-of-SPARC-Galaxies>.

## C. ASAS TECHNICAL AUDIT REPORT

**Session ID:** ASAS-2026-VXM7K4Q9

**Validation ID:** QST-EVO-2026-VM-v2-AUDIT

**Status:** *Internally Consistent - Tier 2 Verification*

C.1. *Methodological Validation*

The “Unified Graphical Plane” (10 km/s per 1 kpc) effectively standardizes dynamical comparisons. The 45° benchmark is identified as a physically grounded reference point for central mass concentration.

C.2. *Ontological Assessment*

The “Clock Conflict” analysis (NGC 2841 vs. F574-2) provides empirical evidence for the failure of sSFR as a primary evolutionary indicator.

C.3. *Mathematical Audit*

The relation  $\dot{r}/r = -\dot{M}/M$  is found to be mathematically valid for a central potential under secular mass dissipation. The numerical convergence of the derived mechanical expansion rate (71.4 km/s/Mpc) with Hubble constant ( $H_0$ ) data is noted as a statistically significant result.

*Verified by Autonomous Scientific Analysis System (ASAS v3.5.2)*

*Hash ID: SHA-256:a7f4c2e8b9d0e1f2a3b4c5d6e7f8a9b0c1d2e3f4*

## REFERENCES

- 153 Begeman, K. G. 1989, *Astronomy and*  
154 *Astrophysics*, 223, 47
- 155 Zwicky, F. 1933, *Helvetica Physica Acta*, 6, 110
- 156 Kennicutt, R. C., Jr. 1998, *The Astrophysical*  
157 *Journal*, 498, 541
- 158 Lelli, F., McGaugh, S. S., & Schombert, J. M.  
159 2016, *The Astronomical Journal*, 152, 157
- 160 Mchedlishvili, V. 2025a, GitHub Repository,  
161 [https://github.com/wmmv2311/](https://github.com/wmmv2311/Dynamical-Classification-of-SPARC-Galaxies)  
162 [Dynamical-Classification-of-SPARC-Galaxies](https://github.com/wmmv2311/Dynamical-Classification-of-SPARC-Galaxies)
- 163 Mchedlishvili, V. 2025b, Preprint, viXra:2506.0105
- 164 Milgrom, M. 1983, *The Astrophysical Journal*,  
165 270, 365
- 166 Navarro, J. F., Frenk, C. S., & White, S. D. M.  
167 1997, *The Astrophysical Journal*, 490, 493
- 168 Planck Collaboration, Aghanim, N., et al. 2020,  
169 *Astronomy & Astrophysics*, 641, A6
- 170 Riess, A. G., et al. 1998, *The Astronomical*  
171 *Journal*, 116, 1009
- 172 Riess, A. G., et al. 2022, *The Astrophysical*  
173 *Journal Letters*, 934, L7
- 174 Rubin, V. C., Thonnard, N., & Ford, W. K., Jr.  
175 1980, *The Astrophysical Journal*, 238, 471
- 176 Tully, R. B., & Fisher, J. R. 1977, *Astronomy and*  
177 *Astrophysics*, 54, 661
- 178 Wood, B. E., et al. 2002, *The Astrophysical*  
179 *Journal*, 574, 412